

Isolation of Two Bioactive *ent*-Kauranoids from the Leaves of  
*Isodon xerophilus*ZHI-YING WENG,<sup>†,‡,§</sup> SHENG-XIONG HUANG,<sup>†,‡</sup> MA-LIN LI,<sup>§</sup> YUE-QIN ZENG,<sup>‡</sup>  
QUAN-BIN HAN,<sup>†</sup> JOSE LUIS RIOS,<sup>\*,‡,⊥</sup> AND HAN-DONG SUN<sup>\*,†</sup>

State Key Laboratory of Phytochemistry and Plant Resources in West China, Kunming Institute of Botany, Chinese Academy of Sciences, Kunming 650204, People's Republic of China; Graduate School of the Chinese Academy of Sciences, Beijing 100039, People's Republic of China; Yunnan Laboratory of Pharmacology for Natural Products, Kunming Medical College, Kunming 650031, Yunnan, People's Republic of China; and Department of Pharmacology, University of Valencia, 46100 Burjassot, Spain

*Isodon xerophilus* has been used as a herbal cold tea for the prevention and treatment of sore throat and inflammation in southernwestern China. A phytochemical study on the ethyl acetate (EtOAc) soluble fraction of *I. xerophilus* leaves led to the isolation of two new *ent*-kauranoids, xerophinoids A (1) and B (2), together with 14 known diterpenoids. The structures of xerophinoids A (1) and B (2) were illustrated using spectroscopic methods including 1D and 2D NMR analyses. To study their biological activities, the effects of xerophinoids A (1) and B (2) on nitrite production, tumor necrosis factor (TNF)- $\alpha$  and interleukin (IL)-1 $\beta$  were examined. In addition, xerophinoids A (1) and B (2) also exhibited potent cytotoxicity against several human tumor cell lines (IC<sub>50</sub> < 11  $\mu$ M), but they had no toxicity on human T-lymphocyte (C8166).

**KEYWORDS:** Anti-inflammation; cytotoxicity; herbal tea; *Isodon xerophilus*; *ent*-kaurane diterpenoid

## INTRODUCTION

*Isodon xerophilus* is a perennial plant widely distributed in southern China. Its leaf is traditionally used to prepare healthy herbal beverages, popularly called "liang cha" or "cold tea". This herbal tea is believed to be a good cold remedy; it helps to treat fever and to reduce the achiness, congestion, and inflammation associated with the common cold. Phytochemical analysis has demonstrated that diterpenoids in *Isodon* species are one group of the most biologically active compounds against inflammation and cancer (1). We have studied over 50 *Isodon* species distributed in China, finding about 500 new diterpenoids (2). Among them, total diterpenoids extracted from *I. xerophilus* are most effective against tumor cells.

It has been found that the EtOAc extract of *I. xerophilus* potently inhibits the growth of various tumor cells including K562, HL-60, HCT, and MKN-28 in vitro (3–7). The objective of the present study was to isolate and identify the structures of two new *ent*-kauranoids, xerophinoids A (1) and B (2), and to investigate their bioactivity toward tumor cell lines and some inflammatory mediators.

## MATERIALS AND METHODS

**General Experimental Procedures.** All melting points were measured on an XRC-1 micro melting point apparatus and are uncorrected. Optical rotations were carried out on a Perkin-Elmer model 241 polarimeter. UV spectra were obtained in a UV 210A spectrometer. IR spectra were measured in a Bio-Rad FTS-135 spectrometer as KBr pellets. 1D and 2D NMR spectra were taken on a Bruker AM-400 or a Bruker DRX-500 NMR spectrometer with TMS as internal standard. Mass spectra were recorded on a VG Auto spec-3000 spectrometer or on a Finnigan MAT 90 instrument. Semipreparative HPLC was performed on an Agilent 1100 liquid chromatograph with a Zorbax SB-C<sub>18</sub>, 9.4 mm  $\times$  25 cm column. Column chromatography was performed on silica gel (200–300 mesh; Qingdao Marine Chemical Inc., Qingdao, People's Republic of China), Lichroprep RP-18 gel (40–63  $\mu$ m, Merck, Darmstadt, Germany), MCI gel (75–150  $\mu$ m, Mitsubishi Chemical Corp., Tokyo, Japan), and Sephadex LH-20 (Pharmacia).

**Plant Material.** The leaves of *I. xerophilus* were collected in Jianshui county of Yunnan Province, People's Republic of China, in October 2003. The identity of plant material was verified by Prof. Zhong-Wen Lin, and a voucher specimen (KIB 98-11-25 Lin) was deposited in the Herbarium of the Department of Taxonomy, Kunming Institute of Botany, Chinese Academy of Sciences.

**Extraction and Isolation.** The dried and powdered leaves (1.5 kg) were extracted with 70% Me<sub>2</sub>CO and filtered. The filtrate was concentrated and extracted with EtOAc and *n*-BuOH successively. The EtOAc layer (50 g) was decolorized on an MCI-gel CHP 20P column (5.0  $\times$  60 cm) with 90% aqueous MeOH and 100% MeOH. The 90% aqueous CH<sub>3</sub>OH fraction (46 g) was chromatographed over a silica gel column (8  $\times$  120 cm) and eluted in a step gradient manner with

\* Corresponding authors [(J. L. R.) e-mail riosjl@uv.es (H.-D.S.) e-mail hdsun@mail.kib.ac.cn].

<sup>†</sup> Kunming Institute of Botany, Chinese Academy of Sciences.

<sup>‡</sup> Graduate School of the Chinese Academy of Sciences.

<sup>§</sup> Kunming Medical College.

<sup>⊥</sup> University of Valencia.

**Table 1.**  $^1\text{H}$  and  $^{13}\text{C}$  NMR Data of Xerophinoids A (1) and B (2) (400 and 100 MHz, in  $\text{C}_5\text{D}_5\text{N}$ ,  $J$  in Hertz)

position	xerophinoid A		xerophinoid B	
	$\delta_{\text{H}}$	$\delta_{\text{C}}$	$\delta_{\text{H}}$	$\delta_{\text{C}}$
1a	1.34 m <sup>a</sup>	35.3	1.98 br d (13.5)	30.1
1b	1.01 m		0.85 dt (13.5, 4.0)	
2a	1.23 <sup>a</sup>	19.3		18.5
2b	1.35 <sup>a</sup>			
3a	1.15 <sup>a</sup>	43.3	1.40 <sup>a</sup>	41.5
3b	1.25 <sup>a</sup>		1.17 m	
4		35.4		34.0
5	1.85 d (13.0)	56.9	1.34 <sup>a</sup>	59.9
6	5.66 d (13.0)	74.0	4.15 dd (10.1, 6.5)	74.8
7		204.5		99.8
8		67.0		62.2
9	2.60 br s	61.2	1.66 dd (12.0, 6.1)	53.1
10		55.5		39.6
11a	5.70 br s	65.9	2.53 m	19.5
11b			1.32 <sup>a</sup>	
12a	2.19 m	36.4	2.28 m	30.8
12b	2.07 m		1.41 m	
13	3.27 m	45.3	3.19 br d (9.4)	44.3
14	4.79 br s	76.0	5.47 br s	73.8
15		199.4		210.0
16		149.0		153.4
17a	6.23 br s	113.3	6.24 br s	119.0
17b	5.39 br s		5.47 br s	
18	1.40 s	35.0	1.25 s	34.2
19	1.09 s	21.4	1.01 s	22.5
20	10.9 s	207.0	5.31 br s	103.6
OAC	1.91 s	168.9		
OMe		21.1	3.44 s	56.3

<sup>a</sup> Overlapped signals.

$\text{CHCl}_3/\text{acetone}$  (1:0 to 0:1, v/v) to yield xerophilus G (2 g) and fractions I–VII: fraction I (254.7 mg), fraction II (807.2 mg), fraction III (5.2 g), fraction IV (2.8 g), fraction V (1.1 g), fraction VI (691.7 mg), and fraction VII (656.7 mg). Fraction III was chromatographed on a silica gel column (5.0  $\times$  60 cm) with petroleum ether/ $\text{Me}_2\text{CO}$  (8:2–1:1, v/v) to give compound 1 (340 mg), rosthoin A (1 g), and eight fractions. Fractions 3, 4, and 5 (total 2.1 g) were subjected to chromatography over RP-18 (column 3.0  $\times$  40 cm) with  $\text{MeOH}/\text{H}_2\text{O}$  (30–100%) to give xerophilus A (24 mg) and xerophilus B (19 mg). Fraction 6 (32 mg) was separated by semipreparative HPLC (50%  $\text{MeOH}/\text{H}_2\text{O}$ ) to yield compounds ponidicin (8 mg) and rabadoterm F (3) (12 mg). Fraction IV was chromatographed on an RP-18 column (3.0  $\times$  40 cm) with  $\text{MeOH}/\text{H}_2\text{O}$  (30–100%), and three fractions were obtained. Fraction 2 (1.2 g) was chromatographed on a silica gel column (3.0  $\times$  30 cm) with petroleum ether/ $\text{Me}_2\text{CO}$  (30:1–10:1, v/v) to give xerophilus H (16 mg), xerophilus K (10 mg), longikaurin B (31 mg), and 10 fractions. Fraction 4 (102.1 mg) was chromatographed on a silica gel column (1.5  $\times$  25 cm) with cyclohexane/isopropyl alcohol (50:1–10:1, v/v) to yield compound 2 (32 mg). Fraction 5 (231.4 mg) was also chromatographed on a silica gel column (2  $\times$  25 cm) with cyclohexane/isopropyl alcohol (50:1–10:1, v/v) to obtain macrocalin B (67 mg) and effusanin A (8 mg). Rubescensin C (11 mg) and rabadoterm D (8 mg) were obtained on a semipreparative HPLC (9.4 mm  $\times$  25 cm column) with 45%  $\text{MeOH}/10\% \text{CH}_3\text{CN}/\text{H}_2\text{O}$  (3 mL/min) from fraction 5. Fraction 8 (27 mg) was separated in a semipreparative HPLC (45%  $\text{MeOH}/10\% \text{CH}_3\text{CN}/\text{H}_2\text{O}$ ) to give rubescensin D (13 mg).

**Xerophinoid A (1).** Compound 1 was named xerophinoid A. Its chemical and physical properties were as follows: white amorphous powder;  $[\alpha]_{\text{D}}^{28}$ ,  $-25.52$  ( $c$  0.15,  $\text{CH}_3\text{OH}$ ); UV  $\lambda_{\text{max}}$  ( $\text{MeOH}$ ) nm (log  $\epsilon$ ), 238 (3.84); IR (KBr)  $\nu_{\text{max}}$   $\text{cm}^{-1}$ , 3467, 2954, 2908, 2848, 1748, 1711–1705, 1647, 1432, 1371, 1232, 1288, 1049, 1014, 960;  $^1\text{H}$  and  $^{13}\text{C}$  NMR data (see Table 1); positive ESIMS,  $m/z$  427  $[\text{M} + \text{Na}]^+$ ; positive HRESIMS  $[\text{M} + \text{Na}]^+$ ,  $m/z$  427.1734 (calcd for  $\text{C}_{22}\text{H}_{30}\text{O}_8\text{Na}$   $[\text{M} + \text{Na}]^+$ , 427.1732).

**Xerophinoid B (2).** Compound 2 was named xerophinoid B. Its chemical and physical properties were as follows: white amorphous powder ( $\text{MeOH}$ );  $[\alpha]_{\text{D}}^{28}$ ,  $-20.49$  ( $c$  0.26,  $\text{CH}_3\text{OH}$ ); UV  $\lambda_{\text{max}}$  ( $\text{MeOH}$ ) nm (log  $\epsilon$ ), 240 (3.92); IR (KBr)  $\nu_{\text{max}}$   $\text{cm}^{-1}$ , 3387, 2948, 2875, 1711, 1643, 1552, 1453, 1369, 1094;  $^1\text{H}$  and  $^{13}\text{C}$  NMR data (see Table 1); positive ESIMS,  $m/z$  401  $[\text{M} + \text{Na}]^+$ ; positive HRESIMS  $[\text{M} + \text{Na}]^+$ ,  $m/z$  401.1943 (calcd for  $\text{C}_{21}\text{H}_{30}\text{O}_8\text{Na}$   $[\text{M} + \text{Na}]^+$ , 401.1940).

**Cytotoxicity.** The cytotoxicity of compounds xerophinoids A and B against murine RAW 264.7 macrophages, rat neutrophils, human leukemia cells (K562, NB4, NB4-R2), solid tumor cells (T-24, Me180, BIU87), rat hematopoietic stem cells (32D), and human T-lymphocyte (C8166) was determined by 3-[4,5-dimethylthiazol-2-yl]-2,5-diphenyltetrazolium bromide (MTT) assay (3). Cells in a 96-well plate were continuously exposed to different concentrations of compounds ( $10^2$ – $10^{-2}$   $\mu\text{M}$ ) for 48 h. The OD of each well was measured on a microplate reader (Bioteck EL-340) at two wavelengths (570 and 630 nm).

**Nitrite Production in Intact RAW 264.7 Macrophages (8).** Murine macrophages RAW 264.7 were cultured in DMEM containing 2 mM L-glutamine, 100 units/mL penicillin, 100  $\mu\text{g}/\text{mL}$  streptomycin, and 10% fetal bovine serum. Cells were removed from the tissue culture flask using a cell scraper and resuspended until a final relation of  $1 \times 10^6$  cells/mL. Nitrite production is assessed as the index of nitric oxide (NO) generation in the induction phase. Macrophages (RAW 264.7) were co-incubated in a 96-well culture plate (200  $\mu\text{L}$ ) with 1  $\mu\text{g}/\text{mL}$  of lipopolysaccharide (LPS) at 37  $^\circ\text{C}$  for 24 h in the presence of test compounds at different concentrations (from 10.0 to 0.05  $\mu\text{M}$ ) or vehicle (phosphate-buffered saline). Nitrites were determined in culture supernatant by Griess reagent. Absorbance was measured at 570 nm using a Labsystems Multiskan EX plate reader (Midland, Canada). Results were expressed in absolute absorbance readings; a decrease indicated a reduction in cell viability.

**Determination of Cytokine Production in RAW 264.7 Macrophages.** Cytokine production was determined according to the protocol described by Kuo et al. (9) with modification. RAW 264.7 macrophages ( $10^6$  cells per well) were co-incubated in a 24-well culture plate (200  $\mu\text{L}$ ) with 1  $\mu\text{g}/\text{mL}$  of LPS at 37  $^\circ\text{C}$  for 3 h. After that, 10  $\mu\text{L}$  of a solution of phytohemagglutinin (PHA, 0.5 mg/mL) was added, and cells incubated at 37  $^\circ\text{C}$  during 24 h for interleukin (IL)-1 $\beta$  or 72 h for tumor necrosis factor (TNF)- $\alpha$ , in the presence of test compounds at different concentrations (10.0–0.05  $\mu\text{M}$ ). Then, plates were centrifuged at 1200 rpm during 5 min for cell sedimentation, and supernatants were collected and assayed for cytokine production by a specific enzyme immunoassay eBioscience (San Diego, CA), according to the manufacturer's instructions.

## RESULTS AND DISCUSSION

Xerophinoid A (1) was obtained as an amorphous powder. The molecular formula  $\text{C}_{22}\text{H}_{30}\text{O}_8$  was deduced from the molecular ion peak at  $m/z$  427  $[\text{M} + \text{Na}]^+$  in ESIMS and NMR data and further confirmed by the HRESIMS ( $m/z$  427.1732  $[\text{M} + \text{Na}]^+$ ). The IR spectrum showed absorption bands due to hydroxyl groups (3467  $\text{cm}^{-1}$ ), carbonyl groups (1748 and 1711  $\text{cm}^{-1}$ ), and a C=C double band (1647  $\text{cm}^{-1}$ ). The  $^1\text{H}$  NMR spectrum displayed three tertiary methyl signals ( $\delta_{\text{H}}$  1.09, 1.40, and 1.90, each 3H, s), two olefin signals ( $\delta_{\text{H}}$  5.39 and 6.23, each 1H, br s), and an aldehyde signal ( $\delta_{\text{H}}$  10.9, s). The  $^{13}\text{C}$  and DEPT NMR spectra revealed a total of 22 carbon signals including 3 methyls, 5 methylenes, 6 methines including 3 oxymethines, 1 double bond, 4 carbonyl groups including 1 aldehyde, and 3 nonoxygenated quaternary carbons. These NMR data together with the molecular formula suggested that xerophinoid A has four rings. Considering the NMR data and the structural types of diterpenoids isolated from *I. xerophilus* previously, xerophinoid A was assigned tentatively as an entkauranoid, which was confirmed by the measurement of extensive 2D NMR data (Figures 1 and 2). In the  $^1\text{H}$ – $^1\text{H}$  COSY and HSQC spectra of xerophinoid A, the proton spin systems H-1/H-2/H-3 and H-9/H-11/H-12/H-13/H-14 were deduced

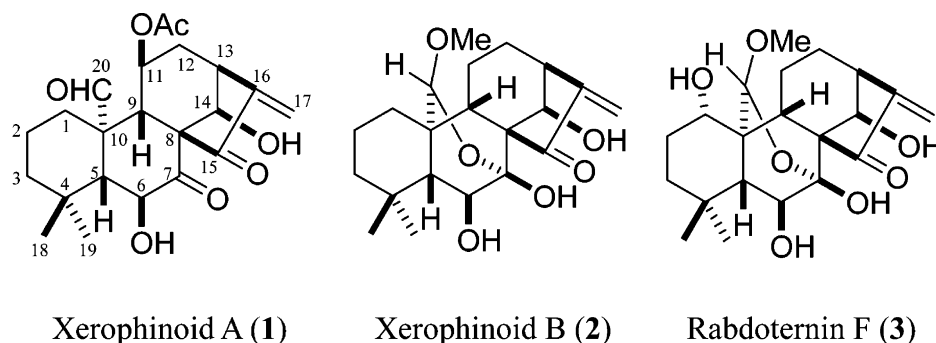


Figure 1. Chemical structures of xerophinoid A (1), xerophinoid B (2), and rabdoternin F (3).

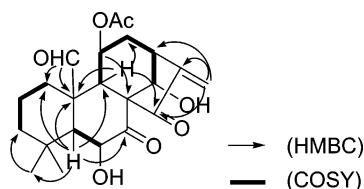


Figure 2. Selected COSY and HMBC correlations of xerophinoid A (1).

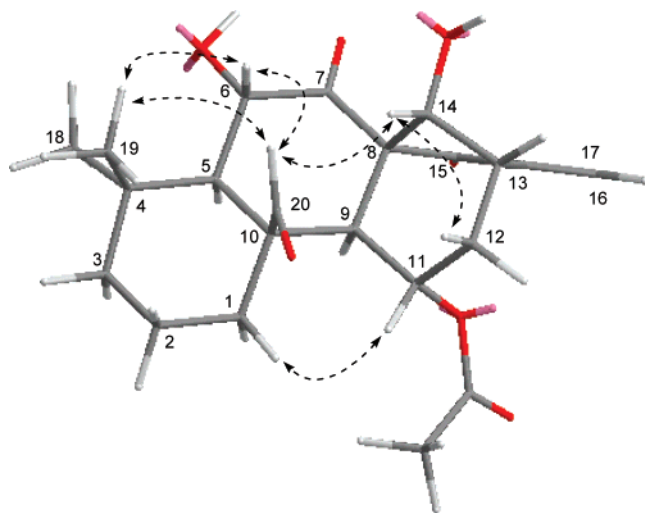


Figure 3. Key ROESY correlations of xerophinoid A (1).

(Figures 1 and 2). Observations of the HMBC correlations of H-5 ( $\delta_H$  1.85 d,  $J$  = 13.0 Hz) with C-1, C-6, C-7, C-9, C-10, C-18, and C-19, H-9 ( $\delta_H$  2.60, br s) with C-8, C-10, C-12, C-14, C-15, and C-20, and H<sub>2</sub>-17 ( $\delta_H$  6.23 and 5.39, each 1H, br s) with C-15, C-16, and C-13 led us to establish the *ent*-kauranoid skeleton. According to the correlations in the HMBC and COSY spectra of xerophinoid A, the acetoxyl group was placed at C-11, the aldehyde was placed at C-20, and two ketone groups were placed at C-7 and C-15, respectively.

The relative stereochemistry of xerophinoid A was deduced from coupling constants and correlations observed in ROESY spectrum as shown in a computer-generated 3D drawing (Figure 3). The trans coupling constant between H-6 and H-5 and ROESY correlations of H-6 with Me-19 and H-20 showed the  $\beta$ -orientation of OH-6. The  $\beta$ -orientation for OH-14 was suggested from the ROESY cross-peak of H-14 with H-20 and H-12 $\alpha$ . The dihedral angles between H-11 and H-9 were close to 90° and 45°, when the 11-OAc group was in an  $\alpha$ - or  $\beta$ -orientation, respectively. Therefore, the coupling constants between H-9 and H-11 could be used in the determination of the relative configuration of C-11 of xerophinoid A. The singlet signal of H-9 indicated that the 11-OAc group was in a  $\beta$ -orientation, which was also supported by the ROESY cor-

relations of H-11 with H-1 $\alpha$ . The absolute configuration of xerophinoid A was not determined experimentally, although it was assumed to belong to the *ent*-series of kaurane. This was the most commonly observed configuration for this class of diterpenoids and appeared to be favored on biogenetic grounds in *Isodon* species. On this basis, xerophinoid A was characterized as 6 $\beta$ ,14 $\beta$ -dihydroxy-11 $\beta$ -acetoxyl-*ent*-kaur-7,15-dioxo-20-al-16-ene.

Xerophinoid B (2) was assigned the molecular formula C<sub>21</sub>H<sub>30</sub>O<sub>6</sub>, as deduced from the positive HRESIMS ( $m/z$  401.1936 [M + Na]<sup>+</sup>). Comparison of the spectroscopic data of xerophinoid B with those of rabdoternin F (3) revealed that they were quite similar except for the moiety at C-1 (Figure 1). Observation of the presence of a methylene carbon ( $\delta_C$  30.1, t) and the absence of an oxymethine carbon in the <sup>1</sup>H and <sup>13</sup>C NMR spectra of xerophinoid B showed that a methylene carbon at C-1 position was evident for xerophinoid B instead of a hydroxyl group at the same position in rabdoternin F (3). Moreover, the correlations in the ROESY spectrum of xerophinoid B indicated that the corresponding substituents in xerophinoid B had the same orientation as those in rabdoternin F (3). Thus, compound xerophinoid B was determined as (20*S*)-6 $\beta$ ,7 $\beta$ ,14 $\beta$ -trihydroxy-20-methoxy-7,20-epoxy-*ent*-kaur-16-en-15-one.

The structures of other compounds isolated were already known, namely, rabdoternin F (10), xerophilus A (3), xerophilus B (3), macrocalin B (11), xerophilus G (12), xerophilus H (12), xerophilus K (5), ponidicin (6), rabdoternin D (5), longikaurin B (5), rosthoriin A (5), effusanin A (13), rubescensin C (14), and rubescensin D (15). The structural identification was made by comparing their spectroscopic data with those in the literature.

Xerophinoids A and B were examined for their cytotoxicity against seven kinds of human tumor cells, human T-lymphocyte (C8166), and rat hematopoietic stem cells (32D). As shown in Table 2, it is noticeable that two new diterpenoids showing cytotoxicity against tested tumor cells except for C8166, T-24, QGY-7202, and BIU-87 cells (IC<sub>50</sub> < 11  $\mu$ M) indicate their broad cytotoxic activities. The IC<sub>50</sub> values against rat hematopoietic stem cells were all <5  $\mu$ M, and that against human T-lymphocyte was >25  $\mu$ M, indicating their side effects should be major in toxicity to hematopoietic stem cells. Xerophinoid B exhibited greater inhibition on K562, NB4, NB4-R2, Me-180, BIU-87, and 32D cells but weaker inhibition on T-24 and QGY-7202 than xerophinoid A. They showed selective cytotoxicity on different human tumor cell lines, which might be due to their different substituents at C-20. In addition, the toxicity of xerophinoid A against murine RAW 264.7 macrophages and rat polymorphonuclear leukocytes was >10  $\mu$ M, whereas thye toxicity of xerophinoid B was >1  $\mu$ M against both cell lines.



**Table 2.** Cytotoxicity of Xerophinoids A (1) and B (2) on Different Cell Lines

cell line	IC <sub>50</sub> <sup>a</sup> (μM)	
	xerophinoid A	xerophinoid B
K562	4.48 ± 1.40	0.32 ± 0.13
NB4	10.09 ± 2.06	3.73 ± 0.67
NB4-R2	3.98 ± 0.87	3.06 ± 0.90
T24	24.59 ± 3.67	45.98 ± 2.31
Me180	5.29 ± 1.34	3.46 ± 0.46
BIU87	40.27 ± 1.94	32.22 ± 3.16
QGY-7202	19.52 ± 1.81	27.06 ± 2.59
32D	4.90 ± 1.31	3.99 ± 0.91
C8166	>25	>25

<sup>a</sup> IC<sub>50</sub> was calculated from the dose response linear regression plots (100–0.01 μM). The results were expressed as mean ± SEM, *n* = 3.

**Table 3.** Inhibitory Effect of Xerophinoids A (1) and B (2) on Production of NO, TNF-α, and IL-β in LPS-Stimulated Cells and in PHA-Stimulated Cells<sup>a</sup>

compound	NO		TNF-α		IL-β	
	%I	IC <sub>50</sub>	%I	IC <sub>50</sub>	%I	IC <sub>50</sub>
xerophinoids A	98**	2.10	41**	>10	100**	<0.05
xerophinoids B	100**	0.24	57**	>1	100**	<0.05
dexamethasone	65**		91**		89**	

<sup>a</sup> Each value represents the mean ± SEM, *n* = 5. Statistical significance of difference from the control: \*\*, *P* < 0.01 (*t* test). %I = percentage of inhibition at 10 μM. IC<sub>50</sub> (μM) was calculated from the dose response linear regression plots (10–0.05 μM). Dexamethasone (10 μM) was used as positive control.

Both new diterpenoids reduced the nitrite production by RAW 264.7 murine macrophages, giving IC<sub>50</sub> values of 2.10 and 0.24 μM, respectively. Moreover, they inhibited the TNF-α production, with an IC<sub>50</sub> < 0.1 μM for xerophinoid B, whereas xerophinoid B inhibited the TNF-α production at concentrations of 10 μM and higher; however, at 0.1 μM and lower concentration, xerophinoid A increased the TNF-α production. Finally, both compounds decreased the IL-1β production, with an IC<sub>50</sub> value of <50 nM.

To date, the research on these compounds has focused only on their cytotoxicity and anticancer activity (5, 16), ignoring their implications in inflammation and immunity. In this regard, Suzuki et al. (16) reported that a related compound, *ent*-11α-hydroxy-16-kauren-15-one, selectively inhibited NF-κB gene expression due to TNF-α treatment. Thus, the joint administration of diterpene and TNF-α increased both the apoptosis in leukemic cells and the activation of caspases. Another structurally related compound, kamebakaurin, strongly inhibited LPS-induced NO production with an IC<sub>50</sub> value of 0.15 μM (17). This effect might be correlated with the inhibition of NF-κB demonstrated by Lee et al. (18), who found kamebakaurin inhibited the NF-κB signal cascade by directly targeting DNA binding of the p50 subunit through a direct covalent modification of cysteine 62. In addition, it inhibited the induced expression of NF-κB target genes encoding the caspase inhibitors c-IAP1 and c-IAP2 and also improved the sensibility of cells to the pro-apoptotic effect of TNF-α. Moreover, Hwang et al. (17) found that a compound closely related to xerophinoid B called kamebacetal (1α-hydroxy derivative of xerophinoid B) inhibited LPS-induced NO production with an IC<sub>50</sub> value of 0.58 μM. The present result demonstrated that xerophinoid B had an IC<sub>50</sub> value of 0.24 μM and that its mechanism of action appeared to be the same as that described above.

The present results, together with previous data obtained for similar compounds, led us to believe that this class of *ent*-kaurane diterpenoids from *I. xerophilus* could be an interesting group of natural products for further development as novel anticancer and anti-inflammatory drugs. The present study provides additional information on the putative mechanism explaining why this herbal tea is beneficial.

## LITERATURE CITED

- (1) Bremner, P.; Heinrich, M. Natural products as targeted modulators of the nuclear factor-κB pathway. *J. Pharm. Pharmacol.* **2002**, *54*, 453–472.
- (2) Sun, H. D.; Huang, S. X.; Han, Q. B. Diterpenoids from *Isodon* species and their biological activities. *Nat. Prod. Rep.* **2006**, *23*, 673–698.
- (3) Hou, A. J.; Li, M. L.; Jiang, B.; Lin, Z. W.; Ji, S. Y.; Zhou, Y. P.; Sun, H. D. New 7,20:14,20-diepoxy *ent*-kauranoids from *Isodon xerophilus*. *J. Nat. Prod.* **2000**, *63*, 599–601.
- (4) Hou, A. J.; Yang, H.; Jiang, B.; Zhao, Q. S.; Liu, Y. Z.; Lin, Z. W.; Sun, H. D. Two new *ent*-kaurane diterpenoids from *Isodon xerophilus*. *Chin. Chem. Lett.* **2000**, *11*, 795–798.
- (5) Hou, A. J.; Zhao, Q. S.; Li, M. L.; Jiang, B.; Lin, Z. W.; Sun, H. D.; Zhou, Y. P.; Lu, Y.; Zheng, Q. T. Cytotoxic 7,20-epoxy *ent*-kauranoids from *Isodon xerophilus*. *Phytochemistry* **2001**, *58*, 179–183.
- (6) Li, S. H.; Niu, X. M.; Peng, L. Y.; Zhang, H. J.; Yao, P.; Sun, H. D. *ent*-Kaurane diterpenoids from the leaves of *Isodon xerophilus*. *Planta Med.* **2002**, *68*, 946–948.
- (7) Niu, X. M.; Li, S. H.; Na, Z.; Lin, Z. W.; Sun, H. D. Two novel *ent*-abietane diterpenoids from *Isodon xerophilus*. *Helv. Chim. Acta* **2004**, *87*, 1951–1957.
- (8) Escandell, J. M.; Recio, M. C.; Mániz, S.; Giner, R. M.; Cerdá-Nicolás, M.; Ríos, J. L. Dihydrocucurbitacin B, isolated from *Cayaponia tayuya*, reduces damage in adjuvant-induced arthritis. *Eur. J. Pharmacol.* **2006**, *532*, 145–154.
- (9) Kuo, Y. C.; Weng, S. C.; Chou, C. J.; Chang, T. T.; Tsai, W. J. Activation and proliferation signals in primary human T lymphocytes inhibited by ergosterol peroxide isolated from *Cordyceps cicadae*. *Br. J. Pharmacol.* **2003**, *40*, 895–906.
- (10) Takeda, Y.; Takeda, K. I.; Fujita, T.; Sun, H. D.; Minami, Y. Rabdotermins D-G, *ent*-7β-20-epoxykaurenes from *Rabdosia ternifolia*. *Phytochemistry* **1994**, *35*, 1513–1516.
- (11) Cheng, P. Y.; Lin, Y. L.; Xu, G. Y. New diterpenoids of *Rabdosia macrocalyx*: the structure of macrocalin A and macrocalin B. *Acta Pharm. Sin.* **1984**, *19*, 593–598.
- (12) Hou, A. J.; Jiang, B.; Yang, H.; Zhao, Q. S.; Lin, Z. W.; Sun, H. D. Three new *ent*-kaurane diterpenoids from *Isodon xerophilus*. *Acta Bot. Yunnanica* **2000**, *22*, 197–200.
- (13) Abbaskhan, A.; Choudhary, M. I.; Tsuda, Y.; Parvez, M.; Attar-Rahman, Shaheen, F.; Parween, Z.; Tareen, R. B.; Zaidi, M. A. A new diepoxy-*ent*-kauranoid, rugosinin, from *Isodon rugosus*. *Planta Med.* **2003**, *69*, 94–96.
- (14) Sun, H. D.; Chao, J. H.; Lin, Z. W.; Marunaka, T.; Minami, Y.; Fujita, T. The structure of rubescensin C: a new minor diterpenoid isolated from *Rabdosia rubescens*. *Chem. Pharm. Bull.* **1982**, *30*, 341–343.
- (15) Sun, H. D.; Zhou, Q. Z.; Fujita, T.; Takeda, Y.; Minami, Y.; Marunaka, T.; Lin, Z. W.; Shen, X. Y. Rubescensin D, a diterpenoid from *Rabdosia rubescens*. *Phytochemistry* **1992**, *31*, 1418–1419.
- (16) Suzuki, I.; Kondoh, M.; Harada, M.; Koizumi, N.; Fujii, M.; Nagashima, F.; Asakawa, Y.; Watanabe, Y. An *ent*-kaurene diterpene enhances apoptosis induced by tumor necrosis factor in human leukemia cells. *Planta Med.* **2004**, *70*, 723–727.

- (17) Hwang, B. Y.; Lee, J. H.; Koo, T. H.; Kim, H. S.; Hong, Y. S.; Ro, J. S.; Lee, K. S.; Lee, J. J. Kaurane diterpenes from *Isodon japonicus* inhibit nitric oxide and prostaglandin E2 production and NF-kappaB activation in LPS-stimulated macrophage RAW264.7 cells. *Planta Med.* **2001**, 67, 406–410.
- (18) Lee, J. H.; Koo, T. H.; Hwang, B. Y.; Lee, J. Kaurane diterpene, kamebakaurin, inhibits NF- $\kappa$  B by directly targeting the DNA-binding activity of p50 and blocks the expression of antiapoptotic NF- $\kappa$  B target genes. *J. Biol. Chem.* **2002**, 277, 18411–18420.

---

**Received for review March 13, 2007. Revised manuscript received May 16, 2007. Accepted May 20, 2007. This study was financially supported by the Natural Science Foundation of Yunnan Province (No. 2004C0008Z) and the National Natural Science Foundation of China (No. 20502026 to Q.-B.H.). Y.-Q.Z. is a recipient of an AECI (Spanish government) grant.**

JF070734W